Focusing of high order harmonics from solid density plasmas

2011 Plasma Phys. Control. Fusion 53 124021

(http://iopscience.iop.org/0741-3335/53/12/124021)

Plasma Phys. Control. Fusion **53** (2011) 124021 (6pp) doi:10.1088/0741-3335/53/12/124021

Focusing of high order harmonics from solid density plasmas

L Waldecker[1,2], P Heissler[1], R Hörlein[1], K Allinger[2], M Heigoldt[1], K Khrennikov[1], J Wenz[1], S Karsch[1,2], F Krausz[1,2] and G D Tsakiris[1]

[1] Max-Planck-Institut für Quantenoptik, D-85748 Garching, Germany
[2] Fakultät für Physik, Ludwig-Maximilians-Universität München, D-85748 Garching, Germany

E-mail: patrick.heissler@mpq.mpg.de

Received 27 June 2011, in final form 1 September 2011
Published 14 November 2011
Online at stacks.iop.org/PPCF/53/124021

Abstract
The generation of coherent radiation in the extreme ultraviolet regime by the interaction of a relativistically intense laser pulse with an over-dense plasma makes a new class of experiments accessible. The availability of isolated attosecond pulses orders of magnitude higher in intensity than those produced in gaseous media would allow for the first time XUV-pump/XUV-probe type experiments with real time resolution on the attosecond timescale. The utilization of these pulses, however, demands complete control over generation and transport parameters. We present a dedicated beamline for generation, transport, application and full characterization of spatial as well as temporal properties of attosecond pulses off solid density targets.

(Some figures in this article are in colour only in the electronic version)

1. Introduction

Short pulse laser systems are nowadays commercially available and widely used in many physics and chemistry groups for time resolved studies with femtosecond resolution. For investigations of processes on even shorter time scales, like e.g. electronic motion within atoms or molecules, pulses with durations below a single cycle of an optical electric field become necessary. Hence, for the composition of these pulses a shift of the central wavelength to the extreme ultraviolet (XUV) or even the soft x-ray regime is inevitable. Today's state of the art technique for the generation of pulses as short as 80 is the interaction of a short, intense laser pulse with a noble gas [1, 2]. This method, however, has its limitations due to depletion of the gas in laser fields exceeding a certain field strength [3] and is thus not easily scalable to higher output intensities. The generation of coherent radiation in the XUV off over-dense plasmas from solid surfaces circumvents this limitation. Here an intense laser pulse is focused on a solid target. A plasma is generated on the surface wherein the laser pulse causes an oscillating motion of the electrons. Two mechanisms are now contributing to the strong

XUV content in the reflected laser radiation. One is called coherent wake emission (CWE) and is dominant at non-relativistic intensities, characterized by a normalized vector potential $a_L^2 = I_L\lambda_L^2/[1.38 \times 10^{18}\,\mathrm{W\,cm^{-2}}\,\mu\,\mathrm{m}^2] < 1$. The electric field component perpendicular to the target surface is accelerating electrons out of the plasma. Some of these electrons are in the next semi cycle, after the electric field changed its sign, accelerated back towards the target. There they are forming bunches of electrons penetrating deep into the plasma and triggering plasma waves in their wake [4, 5]. By linear mode conversion these plasma waves can then themselves emit electromagnetic radiation at their local plasma frequency. The synthesis of these frequencies result in the generation of attosecond bursts of light [6]. The highest achievable light frequency is limited by the maximum plasma frequency available, which is given by the target density. Due to the recurrence of the process once every laser cycle the emitted spectrum consists of harmonics of the carrier frequency of the laser.

The second mechanism is known as a relativistically oscillating mirror (ROM). It is dominant for relativistic laser pulses with $a_L > 1$. Also here the electrons are accelerated by the driving laser field, forcing them to perform an oscillatory motion around the plasma–vacuum interface. Due to the strong electric field the electrons gain velocities close to the speed of light. The incoming laser beam is reflected by this fast oscillating surface and its frequency is upshifted by the Doppler effect [7–10]. This process promises ultra-bright-light pulses with durations on the orders of some tens of attoseconds which can be employed in as-pump/as-probe type experiments. The realization of such experiments demands a precise knowledge of the characteristics of the pulses in use. We show the first results of a dedicated beamline for complete characterization of as-pulses generated on solid surfaces.

2. setup

At the Max Planck Institute of Quantum Optics two laser systems are available for high field experiments. The ATLAS is a conventional Ti : sapphire laser system, delivering at 5 Hz pulses of up to 2 J in energy after compression, at a pulse length of 26 fs. The LWS 20 in contrast is a unique non-collinear optical parametric chirped-pulse amplification system providing pulses of 8 fs in duration and up to 150 mJ in energy before compression at 10 Hz repetition rate [11]. By means of a complex vacuum pipe system both of these pulses can be sent to any of the experimental chambers available.

We are using a 90° off-axis parabolic mirror for focusing the p-polarized beam under an angle of incidence of 45° onto solid density targets (see figure 1). The mirror is coated with a layer of enhanced silver and has an effective focal length of 20 cm, corresponding to $F/2.5$ optic for ATLAS. The standard targets in use are fused silica discs with a diameter of 12 cm and a thickness of 1 cm. By mounting the target on a motorized rotation stage, we can provide a fresh and undamaged piece of glass for every shot. A motorized linear stage, mounted parallel to the target surface shifts the target after every full rotation. Two additional stages, one linear stage parallel to the incoming beam and one rotation stage, make it possible to position the target in the focus of the incoming laser beam and adjust the angle of incidence. The entire assembly of the target is mounted on top of yet another long motorized linear stage. This allows the removal of the target mechanism completely out of the laser beam and to bring in a microscope objective connected to a 14 bit CCD camera for observation and adjustment of the laser focus. Since the focusing parabolic mirror is adjustable in 5 degrees of freedom, x, y and z translation as well as tip and tilt, and also tip and tilt of the mirror before that is tunable, we have full control over the position as well as pointing of the focusing laser beam.

After hitting the target the reflected, diverging beam is recollimated by a 135° off-axis parabolic mirror of uncoated fused silica with a focal length of 13 cm, which sends the beam

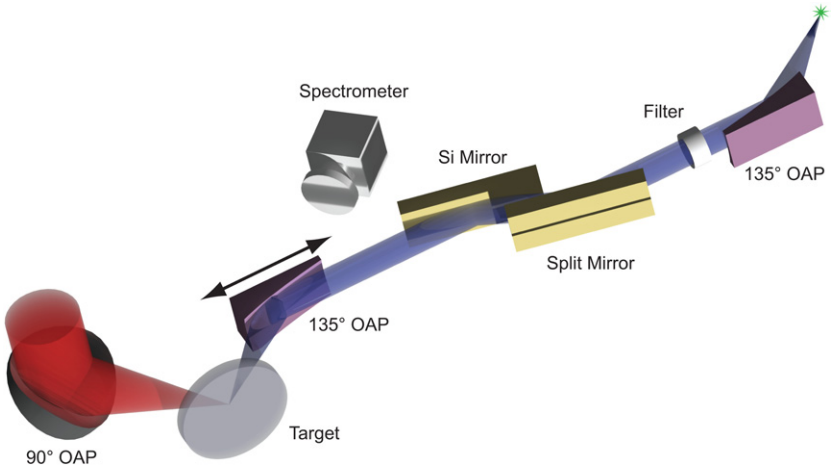

Figure 1. Experimental setup. The generated XUV is recollimated and focused by two identical 135° off-axis parabolic mirrors. Spectral filtering and IR suppression are done by two Si mirrors and changeable filters. A spectrometer allows monitoring spectral properties.

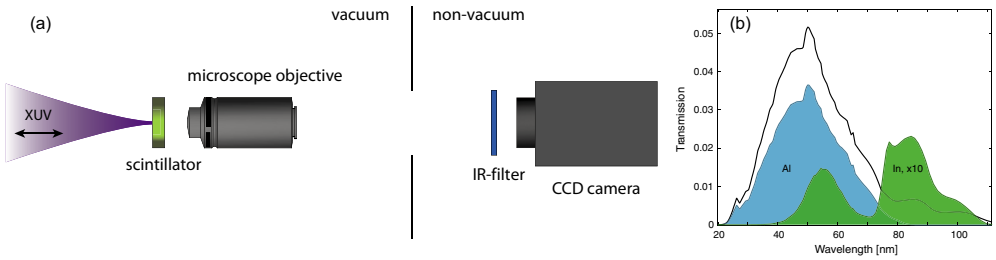

Figure 2. (*a*) System for characterizing the XUV beam. A scintillating crystal shifts the wavelength to the visible range. Magnification is obtained with standard optics. (*b*) Transmission through the setup without (black curve) and with the use of different filters (coloured areas, In magnified by a factor of 10).

into a second vacuum chamber. This parabolic mirror can be moved out of the beam path with a motorized linear stage and the generated radiation can then be analysed by the use of a spectrometer. We have three spectrometers available in this configuration. An Acton VM-502 normal incidence spectrometer ($f/4.5$) and a McPherson grazing incidence XUV-spectrometer ($f/45$) are coupled to the source by means of an appropriate spherical mirror (approximately $f/20$ and $f/10$, respectively), whereas a home built flat-field spectrometer (approximately, $f/20$) equipped with a 1200 lines mm^{-1} Hitachi flat-field grating directly images the source.

With the collimating parabola in use, the beam is next reflected by two Si mirrors. These mirrors are placed at Brewster's angle for the 800 nm central wavelength of the driving laser and therefore act as an efficient IR-suppression unit. The second Si mirror is horizontally cut in the middle, acting as a wavefront beam splitter and thus allows the introduction of a delay into one of the beam halves. Coarse and fine positioning of the upper half are feasible by the use of either a picomotor or a piezo-drive. Subsequently filters can be introduced into the beam path by the use of motorized flippers, before the beam enters the interaction vacuum chamber and is focused by a second 135° parabolic mirror, with the same specifications as the first one. The transmission of the setup is estimated using tabulated data [12, 13] to be higher than 1% in the wavelength range between 30 and 80 nm (see figure 2).

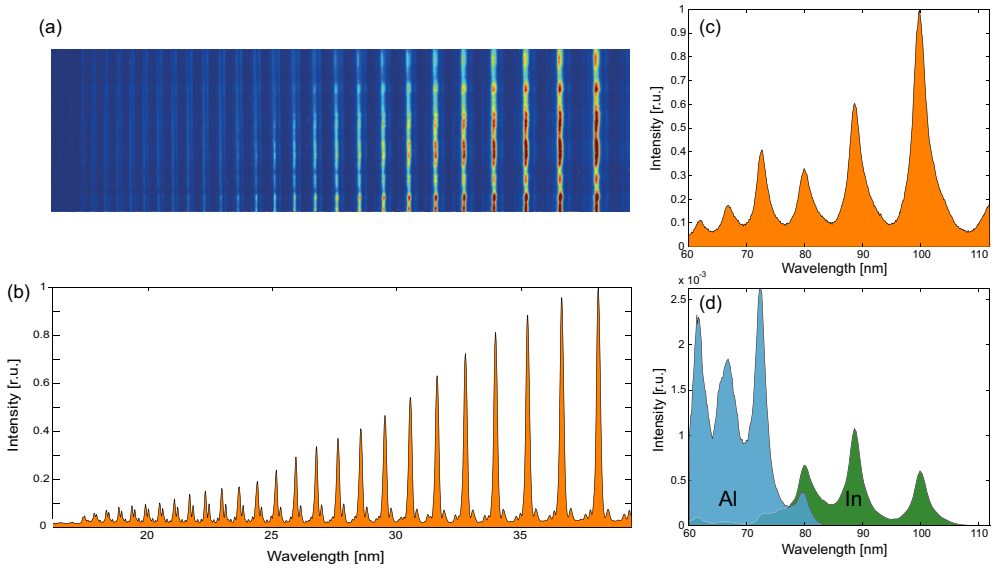

Figure 3. Different spectra obtained with various spectrometers. (*a*) Raw image of a flat-field spectrum with an Al filter (maximum count rate 8241) and (*b*) integrated intensity over all columns. (*c*) spectrum taken with the Acton VM-502 and (*d*) the same spectrum, multiplied with the setup transmission for two filter settings (Al in blue, In in green).

For setup optimization as well as for alignment purposes, it is desirable to be able to directly observe the XUV focal spot in the interaction region. This indeed is not possible by means of standard detectors such as CCDs or MCPs, since the size of the focus is on the order of the pixel size of these instruments thus making magnification necessary. Since transmissive optics in this wavelength range are not available only reflective optics come into consideration, rendering the setup expensive and very complicated. An elegant solution is the use of a scintillating crystal for converting the XUV radiation into visible light allowing the use of standard optical components [14]. We therefore place the front surface of a 100 μm thick YAG : Ce crystal, with a level of doping of 0.15% at the position of the XUV focus and image the fluorescence spot with a microscope objective onto a cooled 16 bit CCD camera resulting in a resolution of about 1 μm. The camera is equipped with a high pass filter to block the residual laser light (see figure 2(*a*)).

3. Measurements

For the measurements we report here, the ATLAS laser system was used but leaving its last two amplification stages inactive. The pulse energy was therefore reduced to approximately 140 mJ on target, while reaching pulse lengths as short as 26 fs. This results in peak intensities of $a_L \approx 5$. In figures 3(*a*) and (*b*) a single shot spectrum recorded with the flat-field spectrometer is shown. Harmonics are observed up to the absorbing edge of the 150 nm thick Al filter at 17 nm. Since the cut-off for the CWE process is expected to be at 40 nm, the spectrum shown is solely produced by the ROM mechanism. In figure 3(*c*) an unfiltered spectrum taken with the Acton spectrometer is shown. The spectral resolution is clearly lower than the one with the flat-field spectrometer. Also no clear statement about the generating mechanism is possible since the CWE cut-off is not observable because of the reduced efficiency at shorter

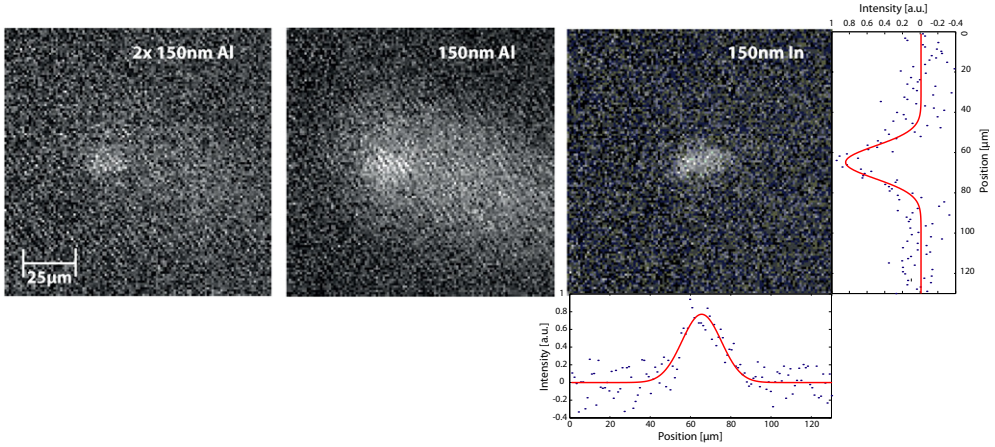

Figure 4. Images of the XUV focus using different filter combinations (all single shot).

wavelength. Multiplying the measured spectrum with the calculated transmission of the setup shows (see figure 3(*d*)) that only a very few harmonic peaks are effectively transmitted with the In filter. In contrast, taking into account the flat-field spectrum, a wide spectral range is transmitted by employing Al filters.

The alignment of the XUV beamline is first checked with the IR beam. The laser intensity is reduced to a low level so as to not damage the target. By rotating the polarization of the laser, thus reducing the suppression on the Si mirrors and removing the high pass filter from the camera the arrangement of the split mirror and the focus of the last parabolic mirror can be optimized. Observing constructive and destructive interference of the two beam halves in the focus allows finding the zero delay of the split mirror to within one pulse length.

Pictures of the single-shot XUV focus for three different filter settings are shown in figure 4. Verification of the XUV nature of the focus is done by placing a glass plate in the beam. While the IR beam is not affected by this plate, the XUV beam is completely absorbed. For Al filters in the beam a small spot surrounded by a big halo can be seen. The small spot can be ascribed to the harmonic spectrum, whereas the large halo is consistent with incoherent line radiation emitted from a much larger region. This is further substantiated by test shots onto previously damaged target spots. Since no clean surface for high harmonic generation is available in these shots, the emission of coherent radiation is efficiently suppressed, but the generation of line radiation due to plasma recombination is still present. This results in the disappearance of the small spot from the signal while the halo can still be seen. Replacing the Al filter by an In filter blocks most of the line radiation in the broadband transmission window of Al and the transmitted spectral range is confined to few low-order harmonics. Fits to the line outs of the small spot yield a harmonic spot size of $d_{\mathrm{FWHM}} = (15.2 \pm 2.1)\,\mu$m. This is larger than expected since the generating laser focal spot size is 2.8 μm and the source size should be even smaller because of the strong intensity dependence of the process [6]. The much larger focus of the harmonics can be explained by saturation of the crystal. Making the conservative assumption of a conversion efficiency of 5×10^{-5} of the laser energy into the harmonics 8–10 and taking into account the losses by transmission through the setup results in a pulse energy of 10^{-8} J focused in the previously mentioned spot size, which in turn is enough to saturate the scintillating crystal. A lower limit for the focused XUV intensity assuming a spot diameter of 16 μm is estimated to be of the order of 2×10^{11} W cm^{-2} using an In filter. Using an Al filter an increase in the focused intensity one to two orders of magnitude is expected.

4. Conclusions

In summary, we have shown the first direct measurements of a focus in the XUV regime generated by harmonics off solid surfaces. The harmonics are well focusable and the intensity in the interaction region is high enough to allow XUV-pump/XUV-probe type experiments. For complete spatial characterization additional devices for direct beam profile and efficiency measurement are ready to be implemented. The temporal characterization will be performed by XUV-FROG type measurements [15] and is also ready to be taken into operation.

Acknowledgments

This work was funded in part by the DFG projects TR-18 and the MAP excellence cluster, by the LASERLAB-EUROPE, grant agreement # 228334, and by the associations EURATOM - MPI fr Plasmaphysik.

References

[1] Hentschel M, Kienberger R, Spielmann C, Reider G A, Milosevic N, Brabec T, Corkum P, Heinzmann U, Drescher M and Krausz F 2001 Attosecond metrology *Nature* **414** 509–13
[2] Goulielmakis E *et al* 2008 Single-cycle nonlinear optics *Science (New York, N.Y.)* **320** 1614–7
[3] Bellini M, Corsi C and Gambino M 2001 Neutral depletion and beam defocusing in harmonic generation from strongly ionized media *Phys. Rev.* A **64** 1–10
[4] Quéré F, Thaury C, Monot P, Dobosz S, Ph Martin Geindre J-P and Audebert P 2006 Coherent wake emission of high-order harmonics from overdense plasmas *Phys. Rev. Lett.* **96** 125004
[5] Thaury C *et al* 2007 Plasma mirrors for ultrahigh-intensity optics *Nature Phys.* **3** 424–9
[6] Nomura Y *et al* 2008 Attosecond phase locking of harmonics emitted from laser-produced plasmas *Nature Phys.* **5** 124–8
[7] Tsakiris G D, Eidmann K, Meyer-ter Vehn J and Krausz F 2006 Route to intense single attosecond pulses *New J. Phys.* **8** 19
[8] Bulanov S V, Naumova N M and F Pegoraro 1994 Interaction of an ultrashort, relativistically strong laser pulse with an overdense plasma *Phys. Plasmas* **1** 745
[9] Gordienko S, Pukhov A, Shorokhov O and Baeva T 2004 Relativistic Doppler effect: universal spectra and zeptosecond pulses *Phys. Rev. Lett.* **93** 1–4
[10] Lichters R, Meyer-ter Vehn J and Pukhov A 1996 Short-pulse laser harmonics from oscillating plasma surfaces driven at relativistic intensity *Phys. Plasmas* **3** 3425
[11] Herrmann D, Veisz L, Tautz R, Tavella F, Schmid K, Pervak V and Krausz F 2009 Generation of sub-three-cycle, 16 TW light pulses by using noncollinear optical parametric chirped-pulse amplification *Opt. Lett.* **34** 2459
[12] Palik E D 1985 *Handbook of Optical Constants of Solids* (New York: Academic)
[13] Henke B L, Gullikson E M and Davis J C 1993 X-ray interactions: photoabsorption, scattering, transmission, and reflection at $E = 50$–$30\,000$ eV, $Z = 1$–92 *At. Data Nucl. Data Tables* **54** 181–342
[14] Valentin C, Douillet D, Kazamias S, Th Lefrou, Grillon G, Augé F, Mullot G, Ph Balcou, Mercère P and Ph Zeitoun 2003 Imaging and quality assessment of high-harmonic focal spots *Opt. Lett.* **28** 1049
[15] Hörlein R *et al* 2010 Temporal characterization of attosecond pulses emitted from solid-density plasmas *New J. Phys.* **12** 043020